Skarn Mineralization along Magma-Carbonate Contacts in the Merry Widow Mountain Area, Vancouver Island, British Columbia (NTS 092L)

R.A. Morris[1], **School of Earth and Ocean Sciences, University of Victoria, Victoria, British Columbia, ramorri@uvic.ca**

D. Canil, School of Earth and Ocean Sciences, University of Victoria, Victoria, British Columbia

Morris, R.A. and Canil, D. (2020): Skarn mineralization along magma-carbonate contacts in the Merry Widow Mountain area, Vancouver Island, British Columbia (NTS 092L); *in* Geoscience BC Summary of Activities 2019: Minerals, Geoscience BC, Report 2020-01, p. 5–12.

Introduction

Wrangellia hosts nearly 50% (~350) of all documented skarn deposits within the Canadian Cordillera, the majority occurring on Vancouver Island (Ray, 2013). Many of these skarn deposits are economically significant and were historically mined for Cu-Au-Co-Ag and Fe (Merry Widow, Kingfisher, Old Sport, Zeballos, Iron Hill and Brynnor; MINFILE 092L 044, 045, 035 and 149; 092F 075 and 001; BC Geological Survey, 2019b).

The past-producing Merry Widow magnetite deposit (Merry Widow Mountain; Figure 1), along with other Fe-skarns in Wrangellia, commonly occur at the contact between intrusions of the Jurassic Bonanza arc and Upper Triassic carbonate rocks of the Quatsino Formation (i.e., the Quatsino limestone) and the Parson Bay Formation. Previous work highlights the association of nearby intrusions with skarn deposits (Sangster, 1964; Ray et al., 1995) but focused mainly on the extent of the mineralization and skarn classification rather than its cause. Attributes such as heat content, bulk composition and cooling history of the magma influence the type and endowment of skarn mineralization but were not the focus of prior studies. This research aims to quantify how these attributes influenced the extent of magma-carbonate reaction and related skarn mineralization. An end goal for this study is to establish the reacted volume per unit time between the magmas and carbonate rocks by investigating which elements are assimilated into the magma and sequestered in the intrusion (the endoskarn). This approach differs from previous efforts that targeted the development of exoskarn (the skarn mineralization that occurs within the wallrock), where most economic deposits are found.

This paper presents the preliminary results from mapping and sampling of the Merry Widow Mountain area during the 2019 summer field campaign. The Merry Widow Mountain area was selected for the initial study as it is easily accessed, has exceptional exposures and displays magma-carbonate interactions on a variety of scales (i.e., broader plutonic-carbonate interactions versus more localized dike-carbonate interactions). The study area is located on northern Vancouver Island, approximately 25 km southeast of Port Alice (Figure 1). Access is by truck from Port Alice along Highway 30 to Alice Lake Road, or via the Keogh Road from Port McNeill. Mapping and sampling were conducted along road cuts and exposures near both active and decommissioned logging roads.

Geological Setting

Wrangellia ranges from Devonian to Jurassic in age and comprises most of the Insular Belt of coastal western Canada. Most units within the terrane were first described by Muller (1977). Wrangellia accounts for the majority (~80%) of the exposed units on Vancouver Island (Figure 1; Muller and Yorath, 1977; Greene et al., 2009). A simplified summary of oldest to youngest stratigraphy on Wrangellia is as follows: Devonian island arc (Sicker Group), Mississippian to Permian siliciclastic and carbonate rocks (Buttle Lake Group), Middle to Upper Triassic large igneous province (Karmutsen Formation), Upper Triassic carbonate rocks (Quatsino Formation; herein referred to as the Quatsino limestone), Upper Triassic to Lower Jurassic calcsilicate and siliciclastic rocks (Parson Bay Formation), and Lower Jurassic arc volcanic rocks and associated intrusions (Bonanza arc; Jones et al., 1977; Muller, 1977; Massey and Friday, 1987; Nixon et al., 1993; Monger and Journeay, 1994; Nixon et al., 1995; Greene et al., 2009). Volcanic and plutonic rocks of the Jurassic Bonanza arc are the youngest units of Wrangellia.

The study area is ~7 km^2 on Merry Widow Mountain (Figure 2). The oldest rocks in the area are volcanic rocks associated with the Karmutsen Formation, just outside the northeastern part of the map area, which underlie the

[1]*The lead author is a 2019 Geoscience BC Scholarship recipient.*

This publication is also available, free of charge, as colour digital files in Adobe Acrobat® PDF format from the Geoscience BC website: http://www.geosciencebc.com/updates/summary-of-activities/.

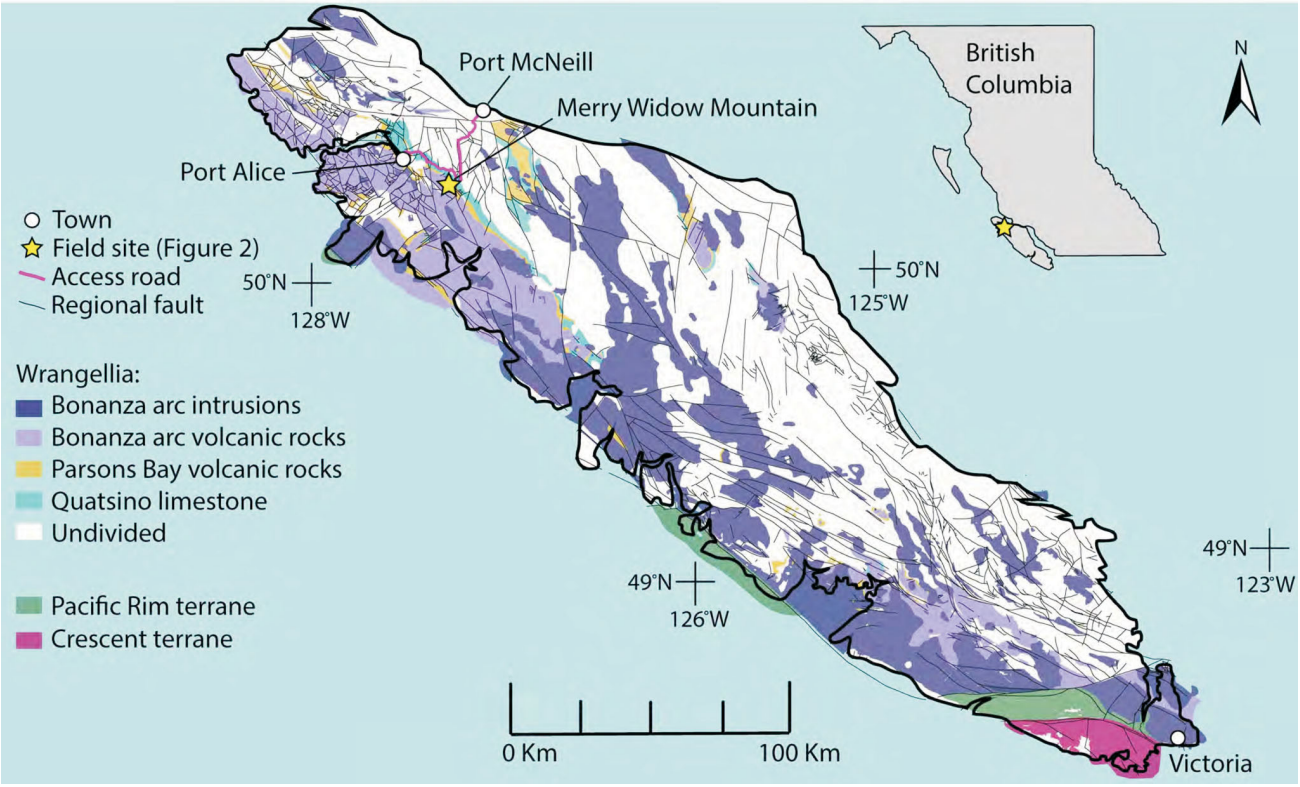

Figure 1. Regional geology of Vancouver Island, showing Wrangellia and the Pacific Rim and Crescent terranes. Wrangellia is stripped of its pre- and post-Jurassic rocks, except for Parson Bay volcanic rocks and Quatsino limestone (both Triassic), which immediately underlie the Jurassic Bonanza arc. Geological-unit boundaries and faults are from the BC Geological Survey (BCGS) MapPlace dataset (BC Geological Survey, 2019a). The Merry Widow Mountain area is located in NTS 092L.

Quatsino limestone (Figure 2; Lund, 1966; Ray and Webster, 1995; Nixon et al., 2011). Measured bedding of the Quatsino limestone and Parson Bay Formation dips gently (~20°) to the west. Mafic dikes crosscut the Quatsino limestone, the Parson Bay Formation (i.e., stratified tuff and volcanic breccia) and the Merry Widow Mountain pluton (Figure 2). Fieldwork was conducted in the eastern region of the Merry Widow Mountain pluton, where it is dominantly gabbroic.

The Merry Widow pit is situated along a prominent northeast-striking (035°), near-vertical fault (the Kingfisher fault) that propagates outward from the pluton margin (Nixon et al., 2011). Most regional faults in the area are near vertical and trend northeast (Figure 2).

Geochronology has been completed on two units within the study area and includes an $^{40}Ar/^{39}Ar$ date of 197.9 ±1.3 Ma on phlogopite within the limestone (presumably contact metamorphosed) and a U-Pb age of 197.1 ±0.3 Ma for zircon within the western region of the Merry Widow pluton (Nixon et al., 2011).

Carbonate

The Quatsino limestone is the oldest and stratigraphically lowermost unit mapped in the Merry Widow Mountain area. It is approximately 1 km in thickness and comprises massive to bedded, grey to white micrite. In some areas, the limestone is locally folded, showing evidence of ductile flow. Folding of the limestone is most apparent within graphite-rich layers (Figure 3a). Regional bedding dips gently (10–30°) to the west. The limestone is crosscut by various dikes and sills (described below) and, in some cases, forms drag folds at the contact with dikes (Figure 3b). These drag folds show evidence of slight normal offset of ~20 cm. Where present, skarn mineralization occurs at the contact of the limestone with dikes and sills, and is usually <25 cm in thickness.

Keystone Intrusion and Associated Dikes and Sills

The Keystone intrusion and associated dikes and sills weather a characteristic light green to buff colour. The groundmass is very fine grained to hypocrystalline. Mafic xenoliths with reaction rims are abundant within the unit and range in size from <1 cm to >20 cm (Figure 4a). Flow banding is common and is parallel to the margins of dikes, or of sills (Figure 4b). Sills follow limestone contacts and dip gently (~20°) to the northwest. Dikes crosscut the limestone bedding and have a moderate to steep southeast dip (~60–75°). Skarn mineralization is most common at contacts of the Keystone intrusion (and associated dikes/sills)

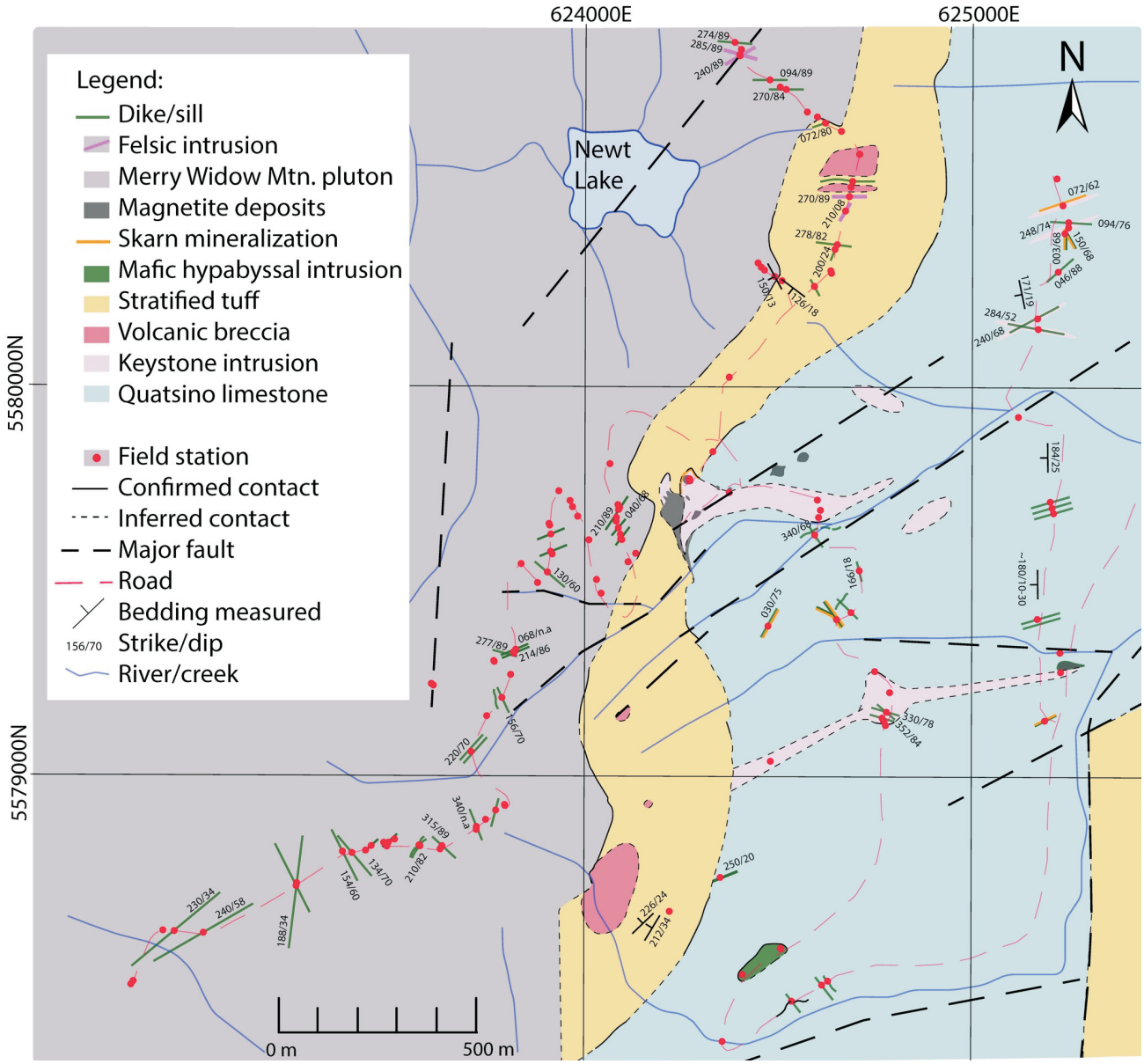

Figure 2. Detailed bedrock geology of the Merry Widow Mountain area, modified after Lund (1966), Ray and Webster (1991) and Nixon et al. (2011). Mapped volcanic breccia locations are from Ray and Webster (1991) and this study (see field stations). The mafic hypabyssal intrusion was previously defined by Ray and Webster (1991) as a pyroxenite. Other previously defined units include the Keystone intrusion (Ray and Webster, 1991) and the Merry Widow Mountain pluton (Nixon et al., 2011).

with the limestone (Figure 4c). The skarn contains assemblages of garnet-diopside-epidote±wollastonite±magnetite (Figure 4c, d). Calcite along the limestone–dike/sill contacts is coarse and frequently recrystallized, and can contain conspicuous void spaces (Figure 4d).

Stratified and Brecciated Volcanic Rocks

Stratified and brecciated volcanic rocks overlying the Quatsino limestone belong to the Parson Bay Formation (Nixon et al., 2011). The stratified unit is a crystal-poor, lithic-rich tuff with a hypocrystalline groundmass, and contains thin layers of quartz-feldspar (Figure 5a). The tuff weathers dominantly light green to buff, with lithic fragments weathering dark grey (Figure 5a). Measured bedding dips gently (~30°) to the northwest. Brecciated volcanic rocks are discordant with the surrounding stratified tuff and occur as near- to subvertical bodies interpreted as subvolcanic plugs (Figure 2). Boundaries between the tuff and volcanic breccia show both brecciation and flow banding. The breccia is polymictic (Figure 5b) and includes clasts that resemble the stratified tuff, plagioclase-phyric basalt and the nearby gabbro (the latter two described below). The groundmass within the breccia is fine grained and weathers dark grey. Previous mapping interpreted the Keystone intrusion (de-

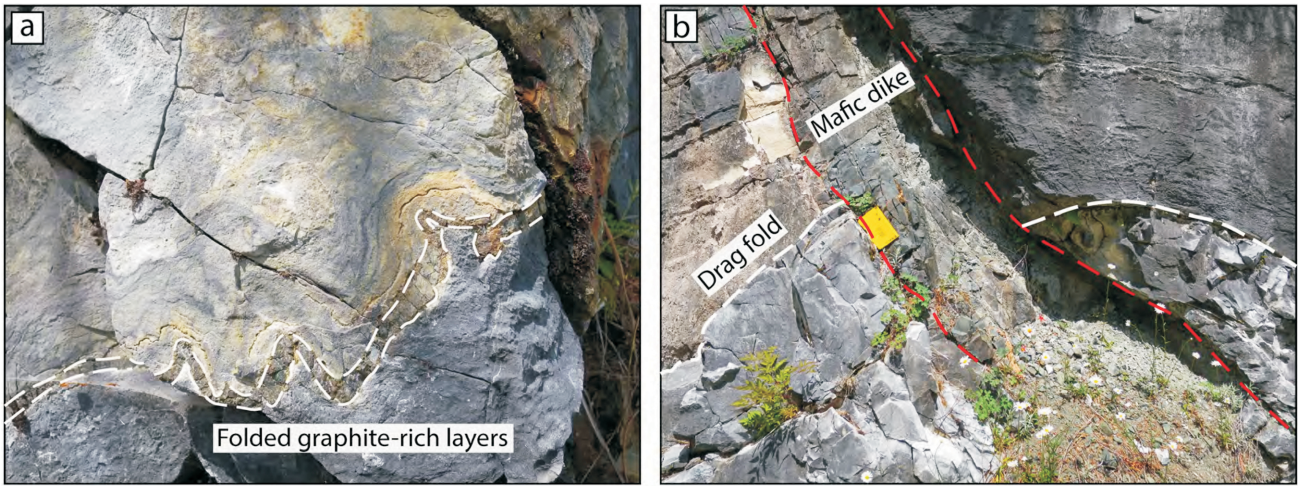

Figure 3. Field images of the Quatsino limestone, displaying **a)** folding of graphite-rich layers (outlined by dashed white line) and ductile behaviour of the surrounding massive limestone; and **b)** drag fold (dashed white line) within the limestone along the contact of a mafic dike (dashed red line); drag fold has a slight normal offset of ~20 cm.

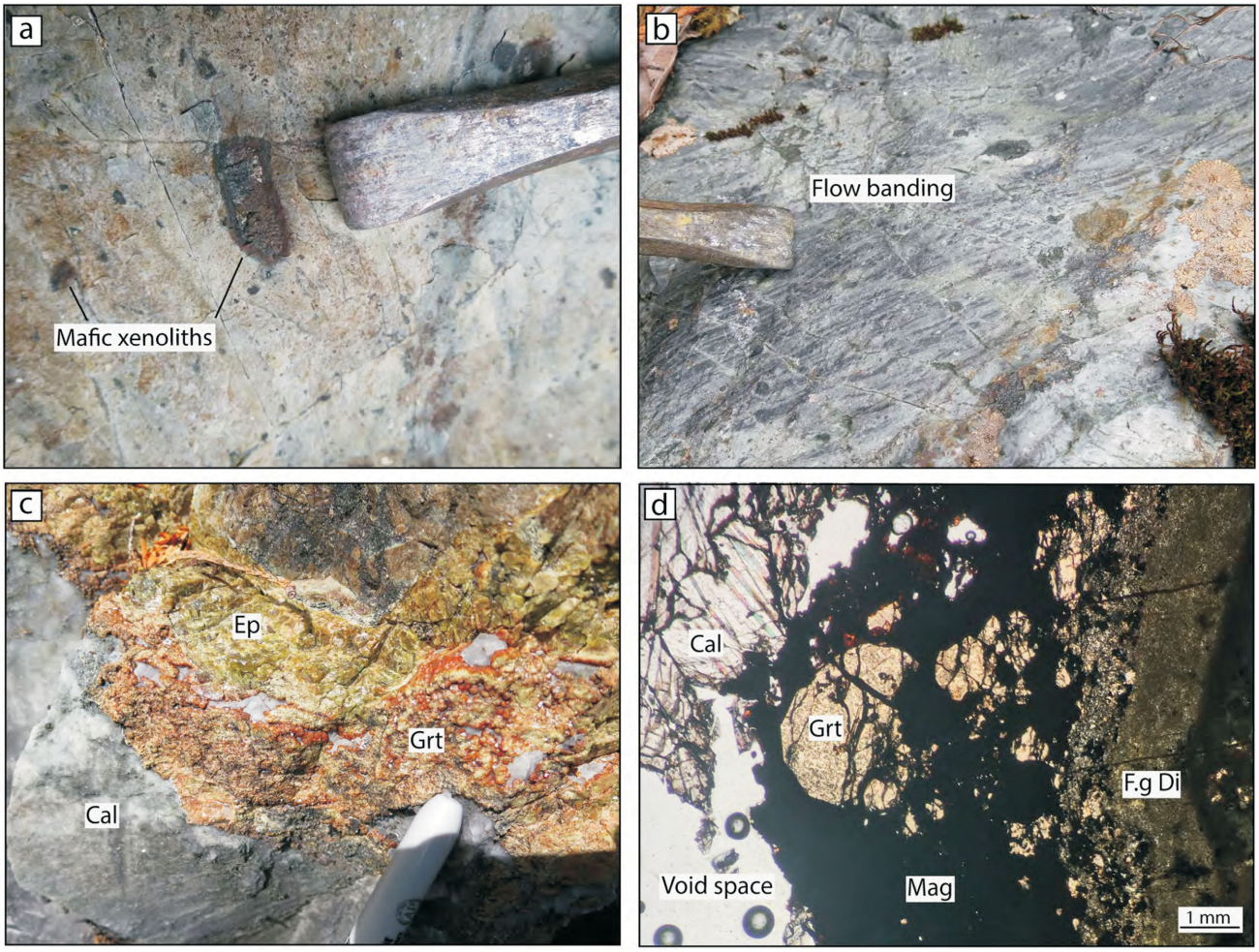

Figure 4. Field and petrographic images of the Keystone intrusion displaying **a)** mafic xenoliths with reaction rims; **b)** flow banding and preferentially oriented xenoliths; **c)** skarn development along the margin of the Keystone intrusion with the limestone (Cal), displaying irregular patches of epidote (Ep) and garnet (Grt); and **d)** the change in mineralogy (Cal-Mag-Grt-Di) shown in plane-polarized light from limestone (Cal) to skarn along the margin of the Keystone intrusion. The calcite is coarse and void spaces are common at the limestone (Cal) to skarn transition. Abbreviations: Cal, calcite; Ep, epidote; F.g. Di, fine-grained diopside; Grt, garnet; Mag, magnetite.

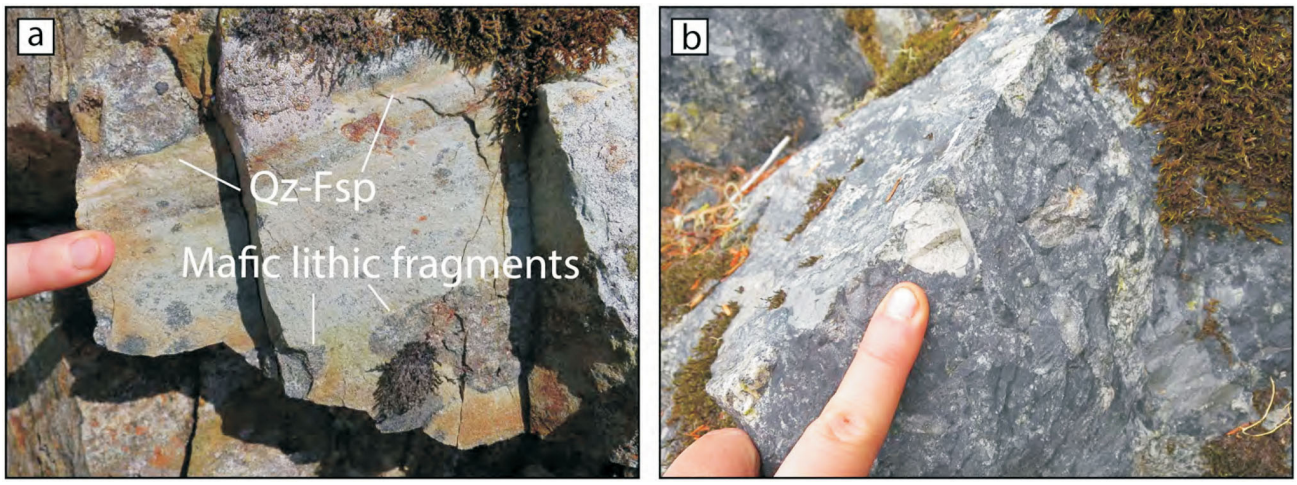

Figure 5. Field images of the Parson Bay Formation, displaying **a)** stratified tuff with thin quartz-feldspar (Qz-Fsp) layers and mafic lithic fragments; and **b)** polymictic volcanic breccia with clasts resembling the stratified tuff, a plagioclase-phyric basalt and the nearby gabbroic intrusion.

scribed above) as the feeder to both the stratified tuff and the volcanic breccia (Ray and Webster, 1991).

Plutonic Rocks

Plutonic rocks of the Merry Widow Mountain area have been previously described as the Coast Copper stock (Ray and Webster, 1991) or the Merry Widow Mountain pluton (Nixon et al., 2011). The present study mapped the eastern margin of the pluton in detail. The pluton is heterogeneous and ranges modally from dominantly gabbro to lesser occurrences of monzonite. Textures display both brittle (sharp, angular boundaries) and ductile (mingling) relationships between the gabbro and monzonite compositions.

The dominant gabbro of the Merry Widow Mountain pluton (Figure 6a, b) is hypidiomorphic, with euhedral plagioclase (45–60%), anhedral clinopyroxene (25–40%), hornblende (<10%), oxides (5–10%), ± olivine (5%). Grain size ranges from medium to pegmatitic, in which euhedral plagioclase crystals can reach up to 5 cm in length. Rare coarse-grained mafic cumulates occur along the margin of the pluton. These cumulates are hypidiomorphic, with altered (i.e., chloritized) hornblende (30%), plagioclase (40%), oxides (10–15%), apatite (5%), clinopyroxene (<5%), olivine (~1–3%) and titanite (~1%). Within these cumulates, apatite grains reaching 2 mm in diameter commonly have melt inclusions (Figure 6c). Titanite typically forms on the edges of apatite (Figure 6c). Fine-grained clinopyroxene along plagioclase boundaries also occurs in some marginal gabbro (Figure 6d).

Mafic Dikes and Sills

In the lower section of the study area, mafic dikes are discordant and sills are concordant with the surrounding limestone bedding (Figure 7a). There is evidence of two sets of dikes/sills. The late dikes/sills form sharp and brittle contacts with the surrounding limestone, whereas the earlier dikes/sills show evidence of ductile deformation at their margins and are commonly boundinaged. Dikes/sills occur as 1) aphyric with microphenocrysts of plagioclase and rare xenoliths that resemble the gabbro; or are 2) plagioclase phyric with euhedral plagioclase laths <1.5 cm in length. Both aphyric and plagioclase-phyric dikes/sills are interpreted to be basalt to basaltic andesite in composition. Aphyric dikes have a steep (~75°) dip to the southeast and the sills have a gentle (<20°) dip to the west. Both aphyric dikes and sills are typically <1–2 m in width. Plagioclase-phyric dikes have a steep (>65°) dip toward either the northeast or southeast and are larger (>2 m in width). Within the lower section of the field area, aphyric dikes commonly cut up through larger, earlier dikes of the Keystone intrusion (i.e., a dike within a dike). Sulphides (chalcopyrite and pyrite) are concentrated along some of these dike contacts with the limestone (Figure 7b).

In the upper section of the study area, mafic dikes crosscut the Merry Widow Mountain pluton (Figure 2). They range from <1 m to >5 m in width and are interpreted to be basalt to basaltic andesite in composition. The dikes dip gently to near vertically (<20° to >80°) between southwest and northwest. The dikes are 1) aphyric with microphenocrysts of plagioclase; 2) plagioclase phyric with euhedral plagioclase laths <1.5 cm in length; or have 3) abundant carbonate-silicate spherules interpreted as ocelli. These ocelli-rich dikes are confined to the upper section where they only crosscut the pluton, and display ocelli amalgamating (Figure 7c) near some of the dike centres. The ocelli are similar in grain size to the groundmass (fine grained) but are lighter in colour (Figure 7c, d). Glomerocrysts of clinopyroxene are common within the ocelli, as well as in the main groundmass. Both the glomerocrysts of clinopyroxene and the ocelli can be up to 3 mm in diameter.

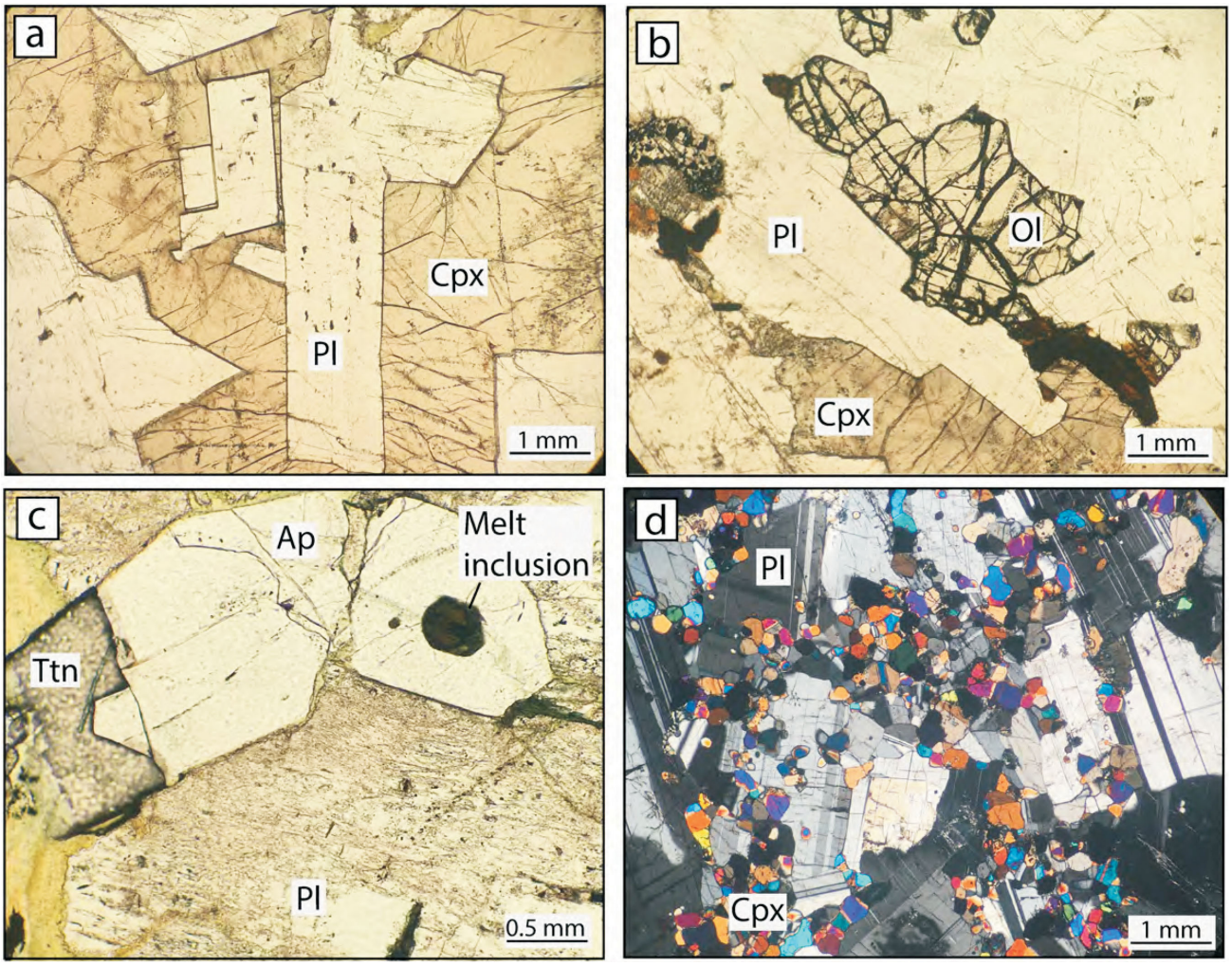

Figure 6. Petrographic images of the gabbro of the Merry Widow Mountain pluton, displaying **a)** euhedral plagioclase (Pl) and anhedral clinopyroxene (Cpx) in plane-polarized light; **b)** euhedral-subhedral olivine (Ol) grains in plane-polarized light; **c)** apatite (Ap) and titanite (Ttn) within mafic cumulates in a marginal gabbro in plane-polarized light; and **d)** fine-grained clinopyroxene (Cpx) along plagioclase (Pl) boundaries in a marginal gabbro in cross-polarized light.

Felsic aplite dikes also crosscut the Merry Widow Mountain pluton and are predominant closer to the plutonic margin and/or near faulted zones (northeast of Newt Lake; Figure 2).

Summary and Future Work

Detailed mapping and sampling during the 2019 summer field campaign in the Merry Widow Mountain area focused on the contacts of the Jurassic Bonanza arc intrusions, dikes and sills with the Quatsino limestone. The overall crustal section dips gently (~20°) to the west and from deepest to shallowest consists of ~1 km of limestone, ~250 m of stratified tuff and volcanic breccia, and ~500 m of gabbro. Skarn development, resulting in garnet-diopside-epidote±wollastonite±magnetite, is most prevalent along contacts between limestone and the Keystone intrusion. Some sulphide concentration (chalcopyrite+pyrite) occurs at the contact between limestone and dikes or sills. No skarn development or sulphide mineralization was observed within the stratified tuff or volcanic breccia. The Merry Widow Mountain pluton is dominantly a plagioclase-clinopyroxene–rich gabbro but displays heterogeneity in composition and texture. Heterogeneity along the margin of the gabbro includes conspicuous coarse-grained mafic cumulates containing abundant apatite (~5%) and occurrences of fine-grained clinopyroxene along plagioclase boundaries. Mafic dikes crosscut all units but have not yet been followed continuously across the exposed depth range. Aphyric and plagioclase-phyric dikes are observed at all levels (i.e., from limestone up to gabbro), whereas mafic dikes containing carbonate-silicate spherules (interpreted as ocelli) are only observed in the upper part of the section, where they crosscut the pluton.

The overarching project goal is to understand all parts of the magmatic system and heat source that led to skarn development at Merry Widow Mountain. It will be important

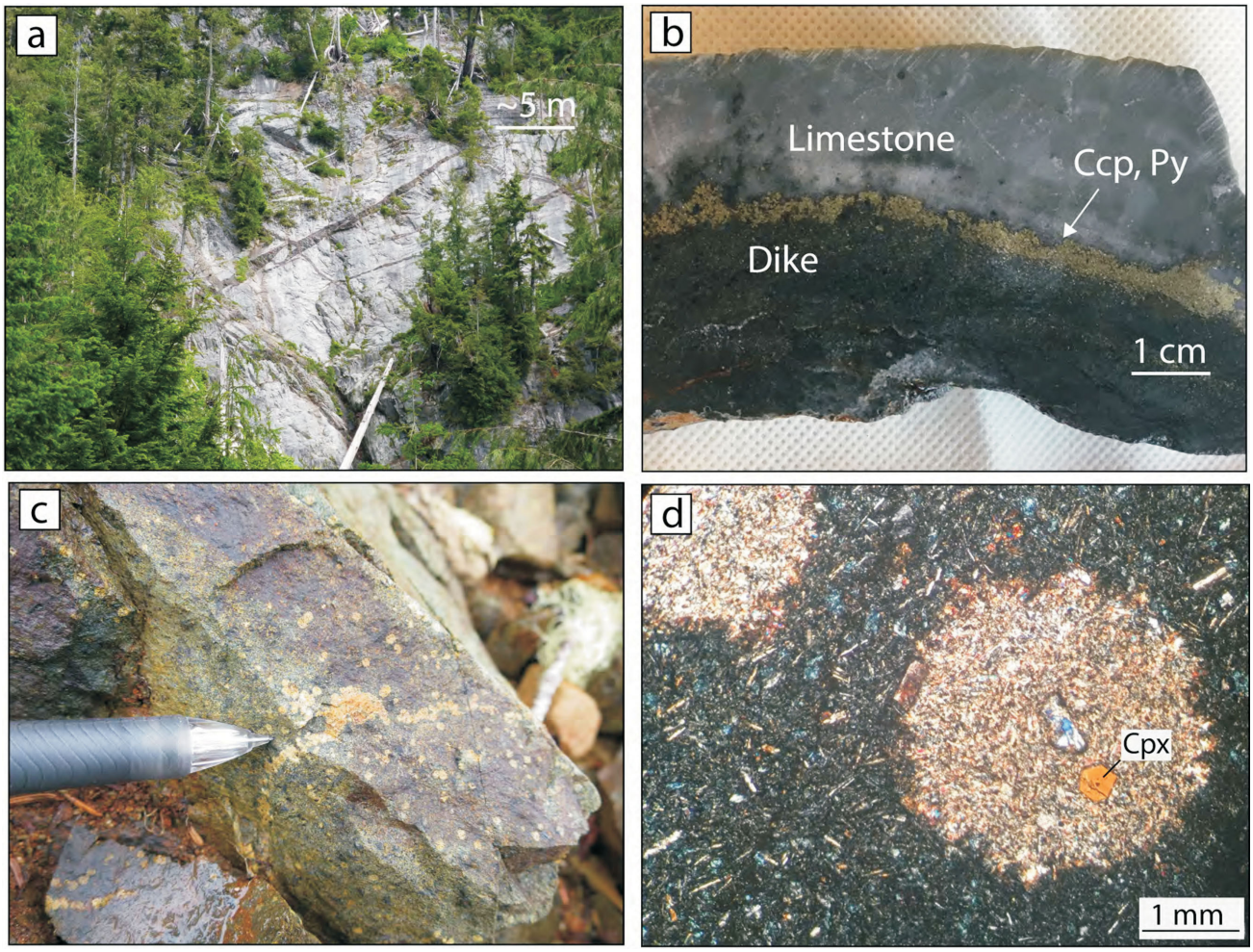

Figure 7. Field and petrographic images displaying **a)** aphyric mafic dikes and sills crosscutting the Quatsino limestone in the lower section; **b)** concentration of chalcopyrite (Ccp) and pyrite (Py) along the margin of an aphyric dike in limestone; **c)** carbonate-silicate spherules interpreted as ocelli amalgamate near the centre of a dike that crosscuts the Merry Widow Mountain pluton; and **d)** ocelli (lighter groundmass, circular) set in a mafic groundmass of similar grain size in cross-polarized light, with a phenocryst of clinopyroxene (Cpx) within one of the ocelli; glomerocrysts of pyroxene can occur within ocelli and in the main groundmass; both ocelli and glomerocrysts can reach up to 3 mm in diameter.

to establish whether the lower dikes that crosscut the limestone and stratified tuffs are related to the upper dikes that crosscut the pluton, and whether either is genetically related to mineralization. Lack of exposures impeded the tracing of dikes upsection into the pluton. It is a priority to complete geochemical analyses on sampled dikes at all crustal levels to identify compositional changes. Geochemical analyses will help assess 1) the extent to which assimilation of limestone into the magma has occurred; 2) the volume and extent of the endoskarn development within the pluton; and 3) relationships (if any) to endoskarn mineralization.

The study will produce details of contact mineralization, and related geochronological data will help to further refine the stratigraphy of Wrangellia, including the ages and groupings of Jurassic plutons and correlations of late Triassic carbonate wallrocks. This research aims to create a predictive tool to aid future exploration for Cu-Au-Co-Ag skarn deposits on Vancouver Island.

Acknowledgments

This project was supported by Geoscience BC scholarships (RM) and a Natural Sciences and Engineering Research Council of Canada (NSERC) Discovery Grant (DC). The authors thank M. Mihalynuk for his thoughtful reviews of this paper.

References

BC Geological Survey (2019a): MapPlace GIS internet mapping system; BC Ministry of Energy, Mines and Petroleum Resources, BC Geological Survey, MapPlace website, URL <http://www.MapPlace.ca> [November 2019].

BC Geological Survey (2019b): MINFILE BC mineral deposits database; BC Ministry of Energy, Mines and Petroleum Re-

sources, BC Geological Survey, URL <http://minfile.ca/> [November 2019].

Greene, A.R., Scoates, J.S., Weis, D., Nixon, G.T. and Kieffer, B. (2009): Melting history and magmatic evolution of basalts and picrites from the accreted Wrangellia oceanic plateau, Vancouver Island, Canada; Journal of Petrology, v. 50, p. 467–505, URL <https://doi.org/10.1093/petrology/egp008> [November 2019].

Jones, D.L., Silberling, N.J. and Hillhouse, J. (1977): Wrangellia – a displaced terrane in northwestern North America; Canadian Journal of Earth Sciences, v. 14, p. 2565–2577, URL <https://doi.org/10.1139/e77-222> [November 2019].

Lund, J.C. (1966): Structural geology of Empire mine, Empire Development Limited, Port McNeil, British Columbia; M.Sc. thesis, University of British Columbia, Vancouver, BC, URL <http://hdl.handle.net/2429/37080> [November 2019].

Massey, N.W.D. and Friday, S.J. (1987): Geology of the Cowichan Lake area, Vancouver Island (92C/16); *in* Geological Fieldwork 1986: A Summary of Field Activities and Current Research; BC Ministry of Energy, Mines and Petroleum Resources, BC Geological Survey Branch, Paper 1987-1, p. 223–229, URL <http://cmscontent.nrs.gov.bc.ca/geoscience/PublicationCatalogue/Paper/BCGS_P1987-01.pdf> [November 2019].

Monger, J.W.H. and Journeay, J.M. (1994): Basement geology and tectonic evolution of the Vancouver region; *in* Geology and Geological Hazards of the Vancouver Region, Southwestern British Columbia, J.W.H. Monger (ed.), Geological Survey of Canada, Bulletin 481, p. 3–25, URL <https://doi.org/10.4095/203245> [November 2019].

Muller, J.E. (1977): Evolution of the Pacific Margin, Vancouver Island, and adjacent regions; Canadian Journal of Earth Sciences, v. 14, p. 2062–2085, URL <https://doi.org/10.1139/e77-176> [November 2019]

Muller, J.E. and Yorath, C.J. (1977): Geology of Vancouver Island; Geological Association of Canada– Mineralogical Association of Canada, Joint Annual Meeting, April 21–24, 1977, Vancouver, BC, Field Trip 7 Guidebook, URL <https://www.gac-cs.ca/publications/FT_Geology_of_Vancouver_Island.pdf> [November 2019].

Nixon, G.T., Hammack, J.L., Hamilton, J. and Jennings, H. (1993): Preliminary geology of the Mahatta Creek area, northern Vancouver Island (92L/5); *in* Geological Fieldwork 1992, BC Ministry of Energy, Mines and Petroleum Resources, BC Geological Survey Branch, Paper 1993-1, p. 17–35, URL <http://cmscontent.nrs.gov.bc.ca/geoscience/PublicationCatalogue/Paper/BCGS_P1993-01.pdf> [November 2019].

Nixon, G.T., Hammack, J.L., Payie, G.J., Snyder, L.D., Archibald, D.A. and Barron, D.J. (1995): Quatsino–San Josef map area, northern Vancouver Island: geological overview (92L/12W, 1021/8, 9); *in* Geological Fieldwork 1994, BC Ministry of Energy, Mines and Petroleum Resources, BC Geological Survey Branch, Paper 1995-1, p. 9–21. URL <http://cmscontent.nrs.gov.bc.ca/geoscience/PublicationCatalogue/Paper/BCGS_P1995-01.pdf> [November 2019].

Nixon, G.T., Snyder, L.D., Payie, G.J., Long, S., Finnie, A., Orr, A.J., Friedman, R.M., Archibald, D.A., Orchard, M.J., Tozer, E.T., Poulton, T.P. and Haggart, J.W. (2011): Geology, geochronology, lithogeochemistry and metamorphism of the Alice Lake area, northern Vancouver Island, NTS 092L/06 and part of 092L/03; BC Ministry of Energy, Mines and Petroleum Resources, BC Geological Survey, Geoscience Map 2011-4, 1:50 000, URL <http://cmscontent.nrs.gov.bc.ca/geoscience/PublicationCatalogue/GeoscienceMap/BCGS_GM2011-04.pdf> [November 2019].

Ray, G.E. (2013): A review of skarns in the Canadian Cordillera; BC Ministry of Energy, Mines and Petroleum Resources, BC Geological Survey, Open File 2013-08, 50 p., URL <http://cmscontent.nrs.gov.bc.ca/geoscience/PublicationCatalogue/OpenFile/BCGS_OF2013-08.pdf> [November 2019].

Ray, G.E. and Webster, I.C.L. (1991): Geology and mineral occurrences of the Merry Widow skarn camp, northern Vancouver Island; BC Ministry of Energy, Mines and Petroleum Resources, BC Geological Survey, Open File 1991-08, 1:5000 scale map, URL <http://cmscontent.nrs.gov.bc.ca/geoscience/PublicationCatalogue/OpenFile/BCGS_OF1991-08.pdf> [November 2019].

Ray, G.E., Webster, I.C.L. and Ettlinger, A.D. (1995): The distribution of skarns in British Columbia and the chemistry and ages of their related plutonic rocks; Economic Geology, v. 90, p. 920–937, URL <https://doi.org/10.2113/gsecongeo.90.4.920> [November 2019].

Sangster, D.F. (1964): The contact metasomatic magnetite deposits of southwestern British Columbia; Ph.D. thesis, University of British Columbia, Vancouver, BC, URL <http://hdl.handle.net/2429/38943> [November 2019].